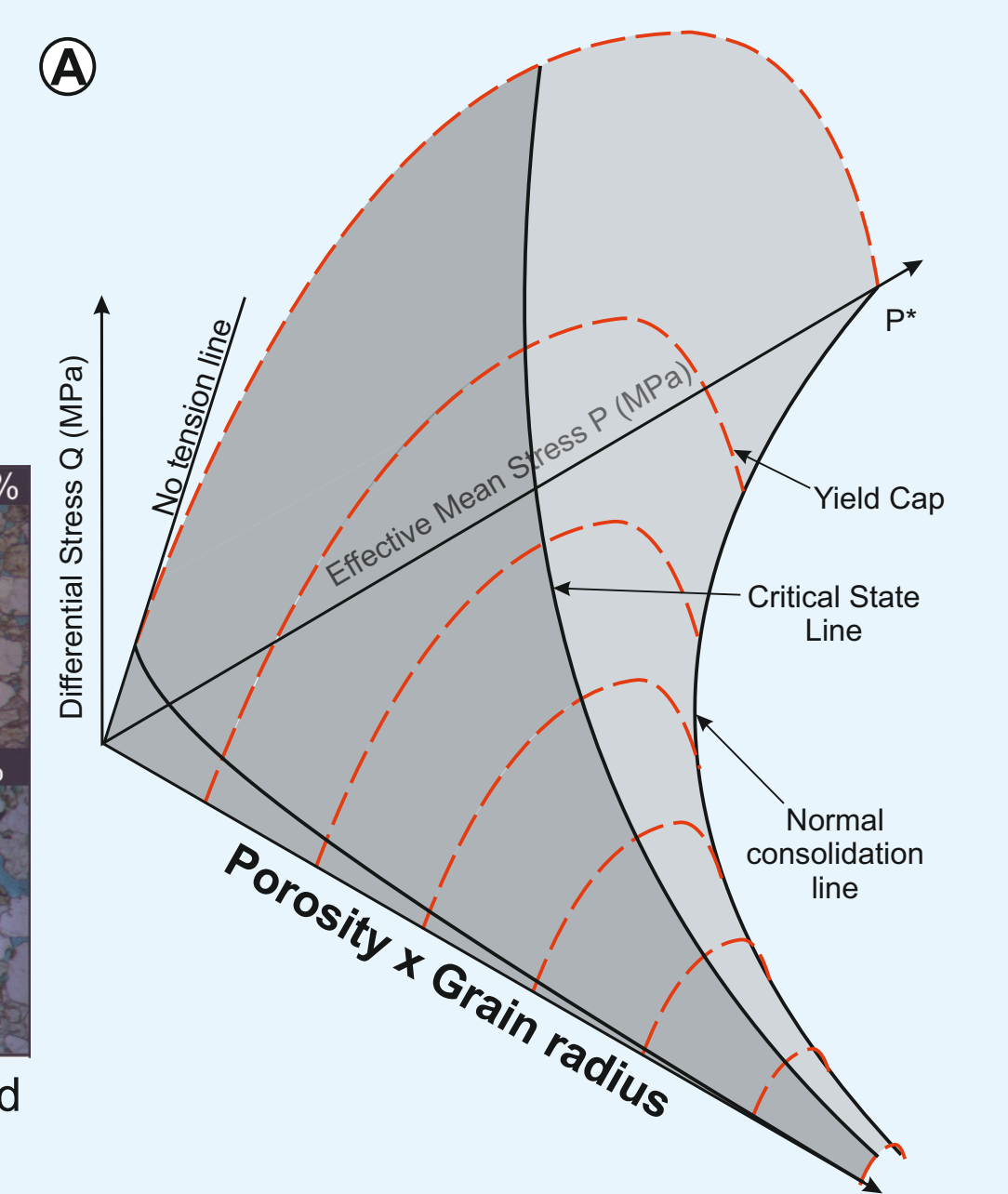
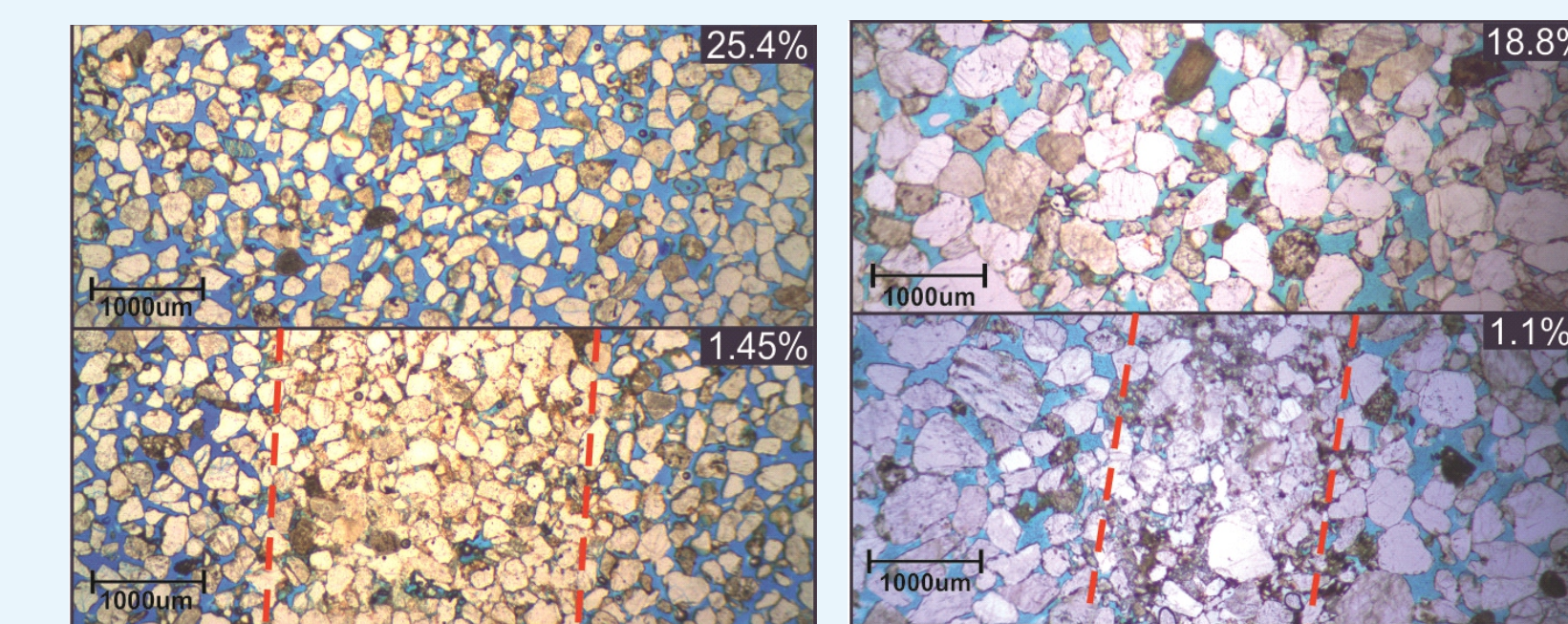


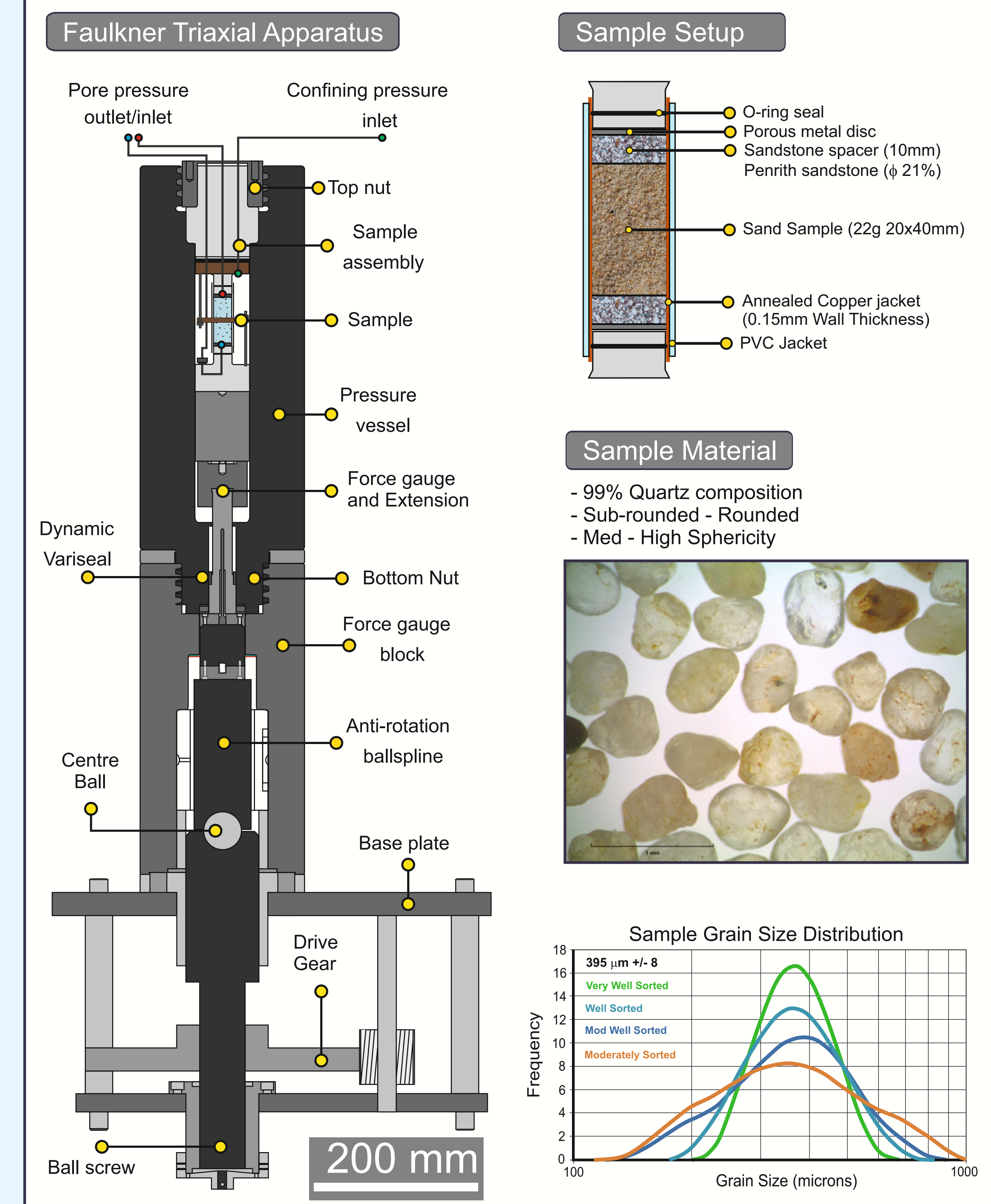
1 Introduction

Deformation bands are the main structural element of fault damage zones within sandstone reservoirs. The prediction of band occurrence and their petrophysical impacts is based largely on the understanding that the yield and deformation mechanism of sandstones is primarily controlled by porosity and mean grain size (figure a). The effect of grain sorting on the mechanical behaviour of sandstones is not well understood, although it is generally regarded that deformation band formation is inhibited in texturally immature sandstones with a poor level of sorting. We examine the effect of sorting on the inelastic yield of sandstones, and the petrophysical impacts of deformation, using a series of triaxial deformation experiments on unconsolidated pure quartz sands.



2 Experimental Setup

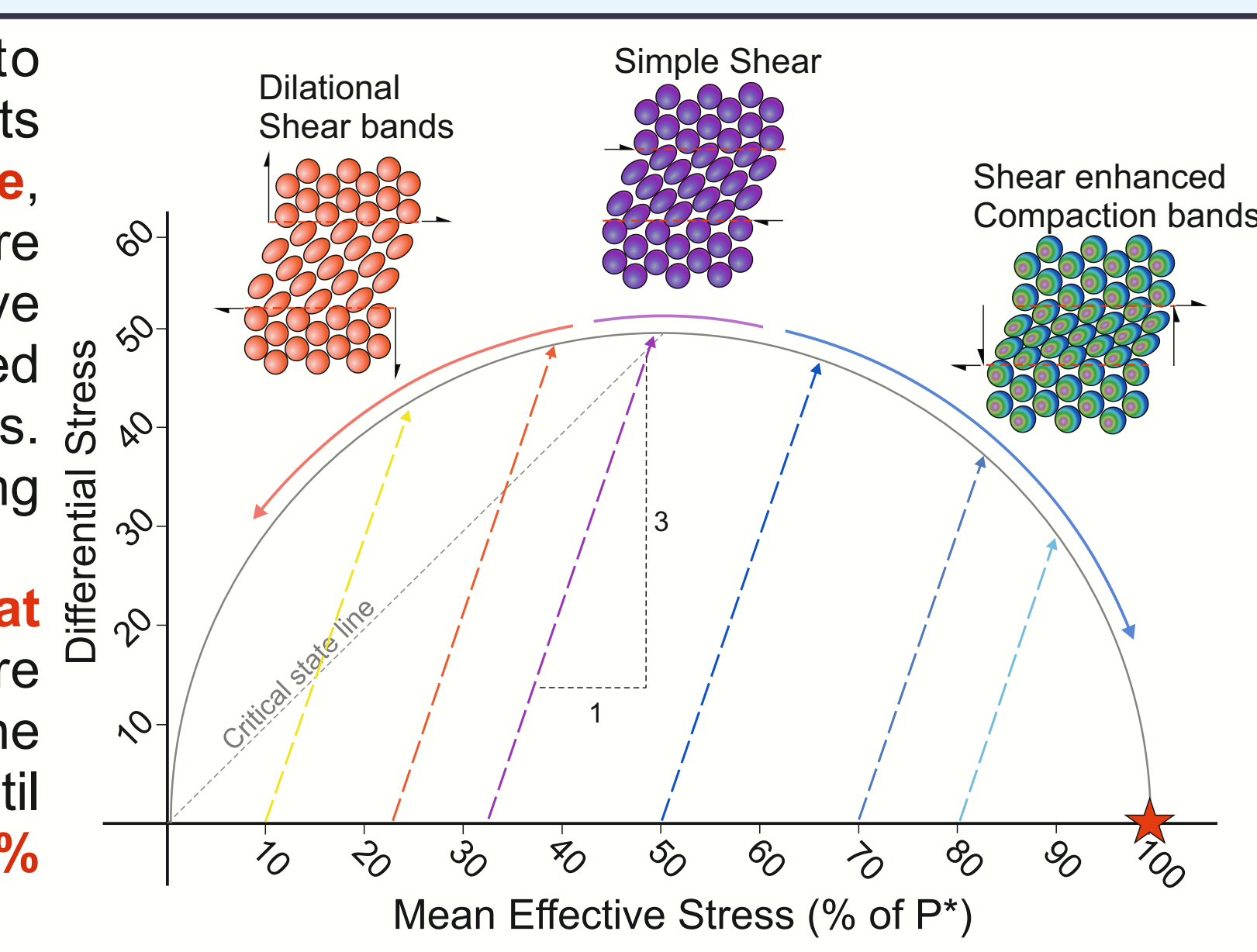
The triaxial apparatus has 250 MPa confining pressure, and 200 MPa pore pressure capability, and is able to load samples axially up to 300 kN. The confining pressure and pore pressure is servo controlled for precision of 0.01 MPa. Pore volume is also monitored during deformation to a resolution of 0.1 mm³. **Samples of quartz sand are contained within annealed copper jackets, capped at both ends with a strong and permeable sandstone.** An additional PVC jacket surrounds the sample. The sample material is a 99% pure quartz sand from the Chelford Formation². Sand was sieved into 100 micron bins which were then passed through a Laser Particle Size Analyser (LPSA). Mixing of these sands allowed us to create four samples with a desired grain size and level of sorting for testing.



3 Methodology

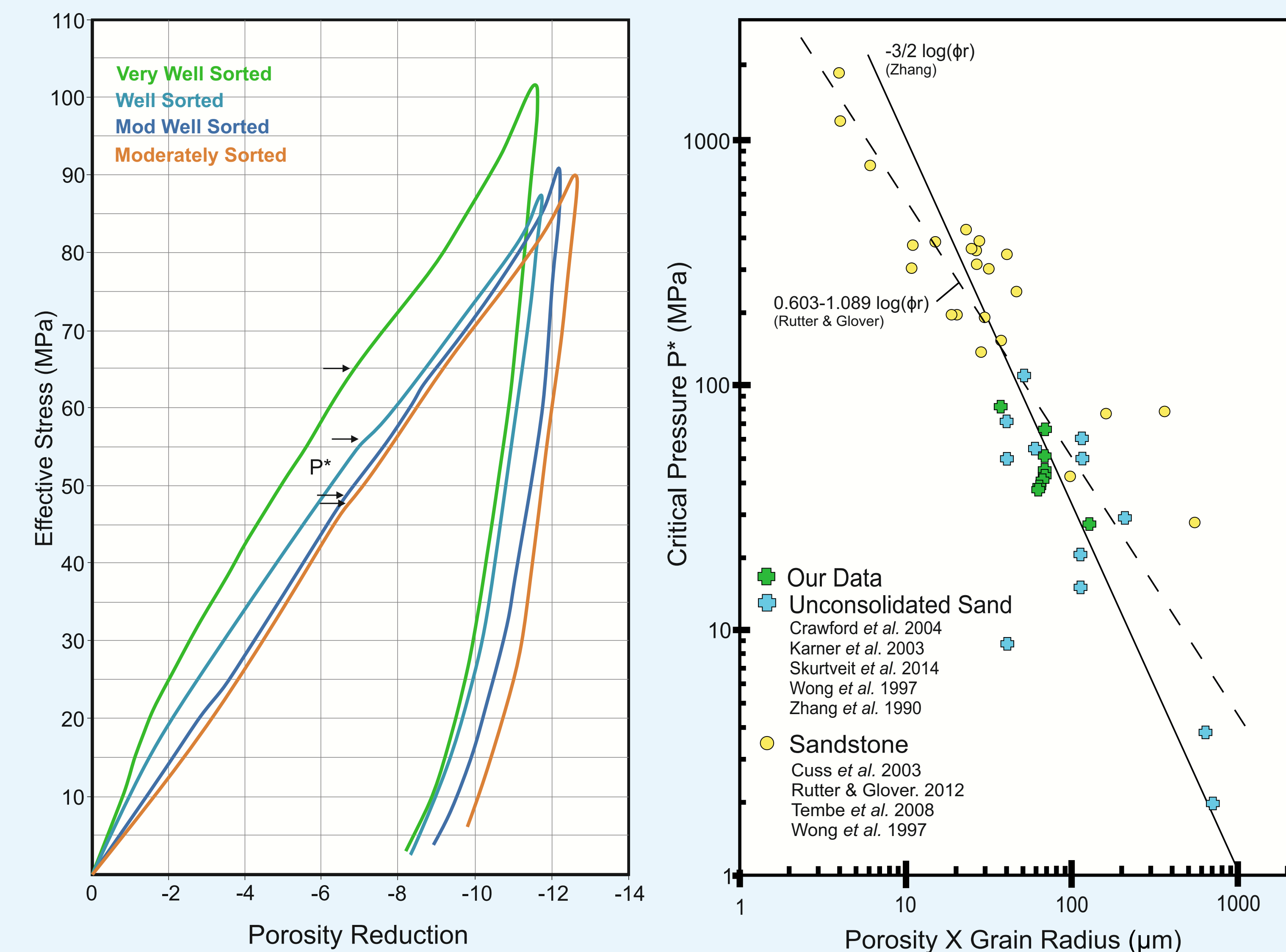
Hydrostatic tests are first performed to establish the grain crushing strength (P^*). Tests are performed with **10 MPa pore pressure**, and loaded incrementally (5 MPa) once pore volume has equalised, to a maximum effective pressure of up to 100 MPa. With P^* established we are able to strategise axial loading tests. Samples are axially loaded at specific confining pressures until failure.

Confining conditions for axial loading are at 10, 22, 32, 50, 70 and 80% of P^* . Pore pressure is held constant at 10 MPa, and the sample is axially loaded at a rate of **1 μ m/s** until C/C^* is observed, and further loaded until **5% axial strain** is achieved.



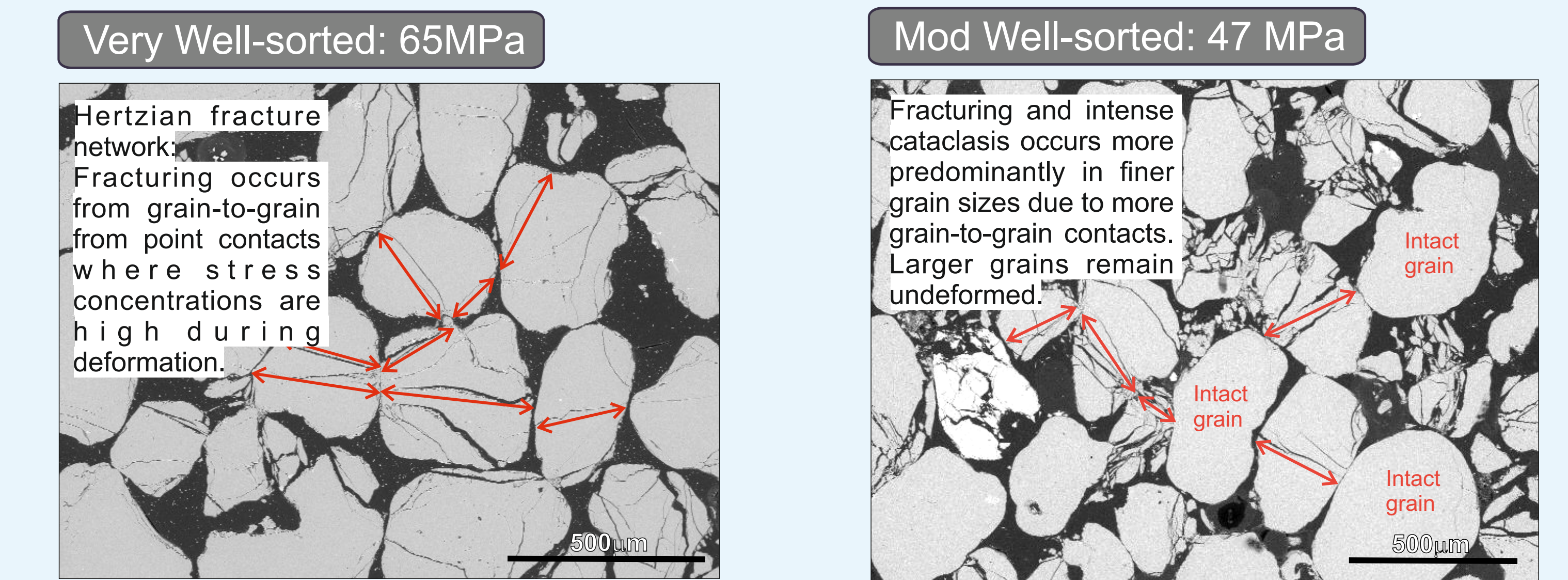
4 Hydrostatic Results

Hydrostatic deformation tests were performed to establish the critical effective pressure (P^*) at which grain crushing occurs. The onset of grain crushing scales with porosity and grain size with the relationship $-3/2 \log(\phi r)$ established by Zhang³, giving us a **calculated P^* of 66-69 MPa** for all tested samples. Hydrostatic tests of four samples with sorting varied from very well sorted (0.3Phi) to moderately sorted (0.6Phi) are plotted below. P^* values obtained from hydrostatic tests are also plotted against porosity x grain radius for comparison with published results.



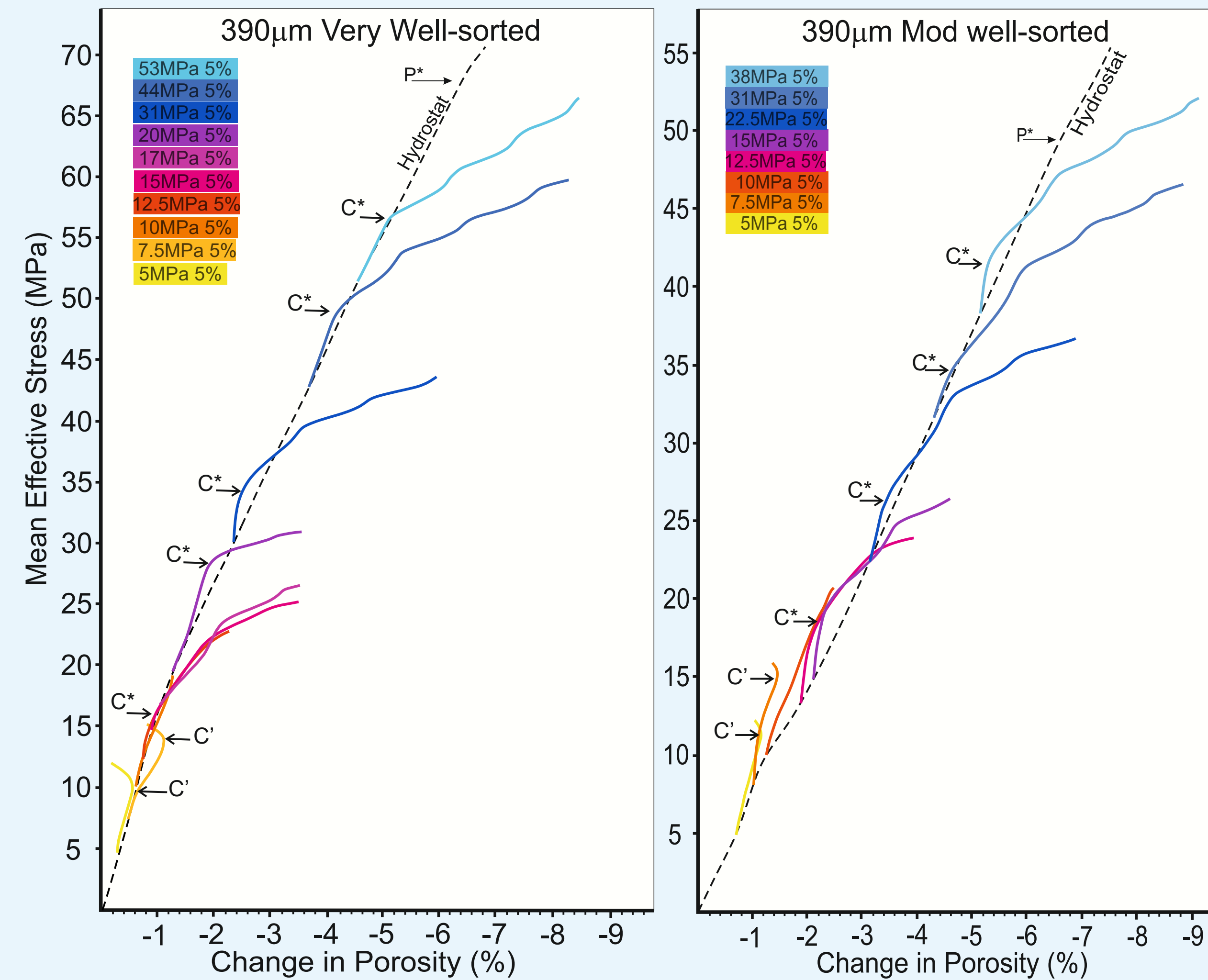
Results of compaction of four samples show very subtle inflections indicating P^* , the onset of grain crushing. Values are higher for well sorted vs poorly sorted samples, **65 to 47 MPa** respectively. Reduction of porosity is approx 2% more for poorly sorted sands, attributed to better packing arrangement during compaction.

Values for the critical pressure (P^*) are **Well predicted by the grain size-porosity relationship** proposed by Zhang, and fit the trend well. Sandstones better fit the trend and relationship proposed by Rutter et al⁴. The differences of which may indicate the subtle effect of cementation of the rock.

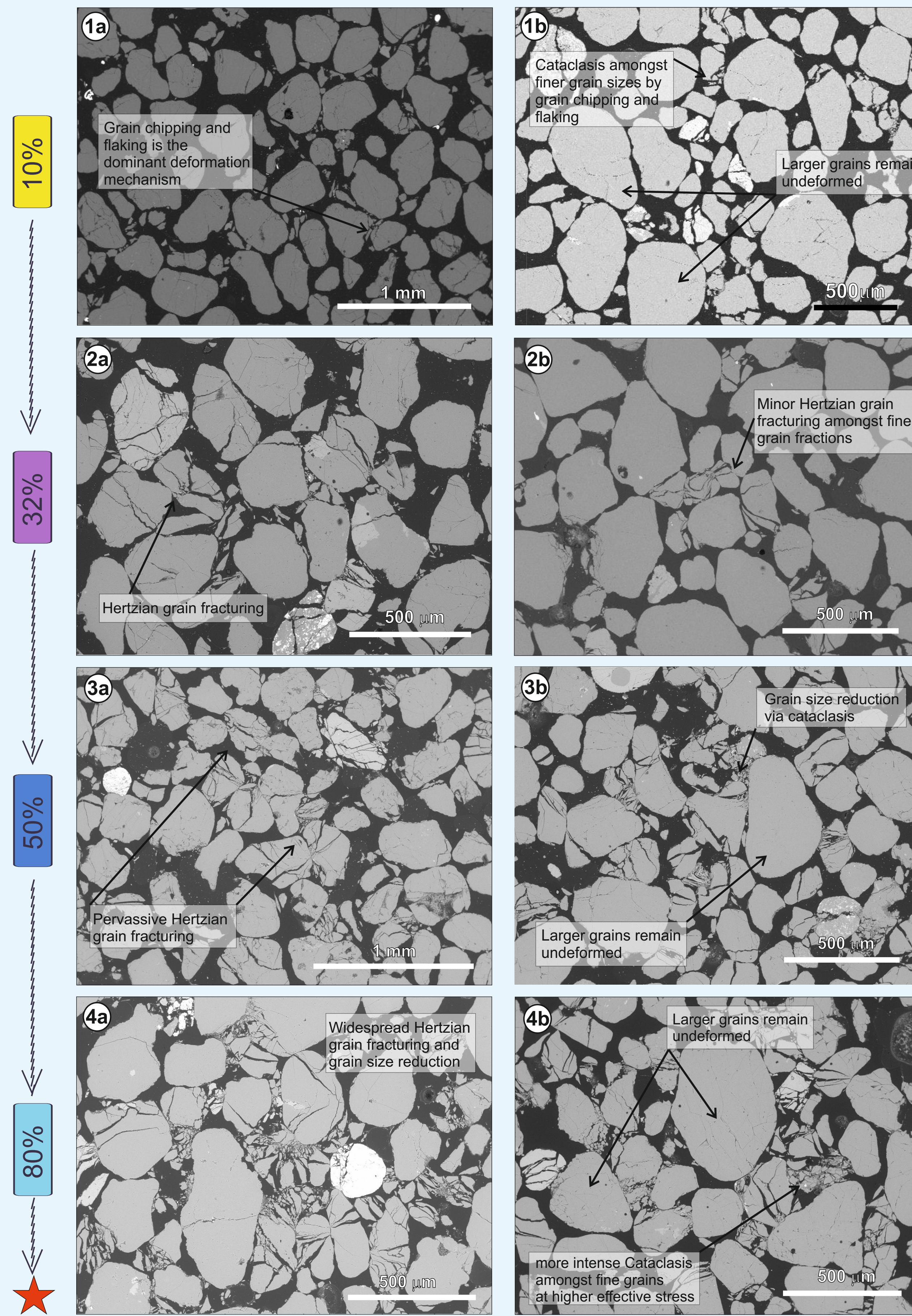


The occurrence of P^* in both our sands can be confirmed by grain crushing in BSE images. Hydrostats indicate sample failure at **65 MPa and 47 MPa** for very well-sorted and moderately well-sorted sands respectively. Both samples show pervasive grain crushing and Hertzian⁵ grain-grain fracture networks (red arrows) that emanate from grain contacts.

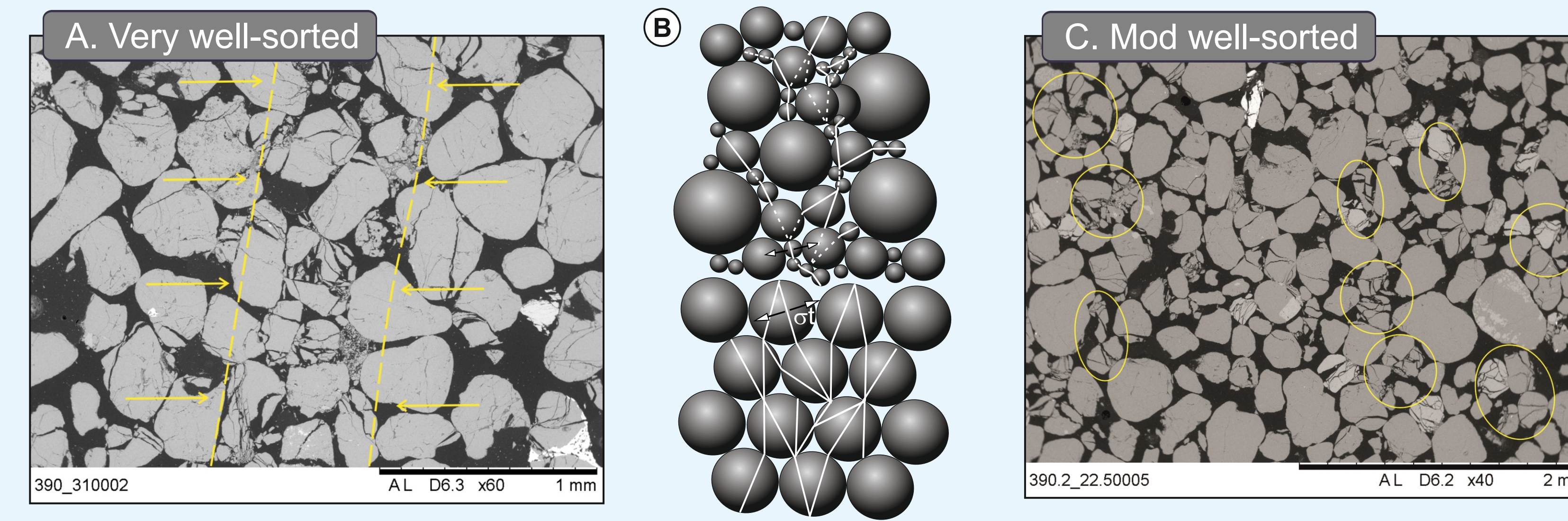
5 Triaxial Tests



Results of tests are plotted above as porosity change vs mean effective stress. **At low confining pressures (7-15% of P^*)** failure is indicated by deviation from the hydrostat, C^* , with **initial porosity loss followed by dilation**. **At higher pressures (>22% of P^*)** failure at C^* results in **significant porosity loss**. Results of tests at **10, 32, 50 and 80%** are shown below. Deformation at low effective pressures is characterised by **grain chipping and flaking** (figure 1a and 1b), transitioning at higher effective pressures to **Hertzian grain fracturing** (figures 2a and 2b, 3a and 3b). At the highest effective stresses (80%) **Intense grain size reduction due to cataclasis is observed** (figures 4a and 4b). Cataclasis is more dominant and pervasive in the well sorted sands. In poorly sorted sands, cataclasis occurs amongst finer grain fractions, leaving larger outliers largely undeformed.

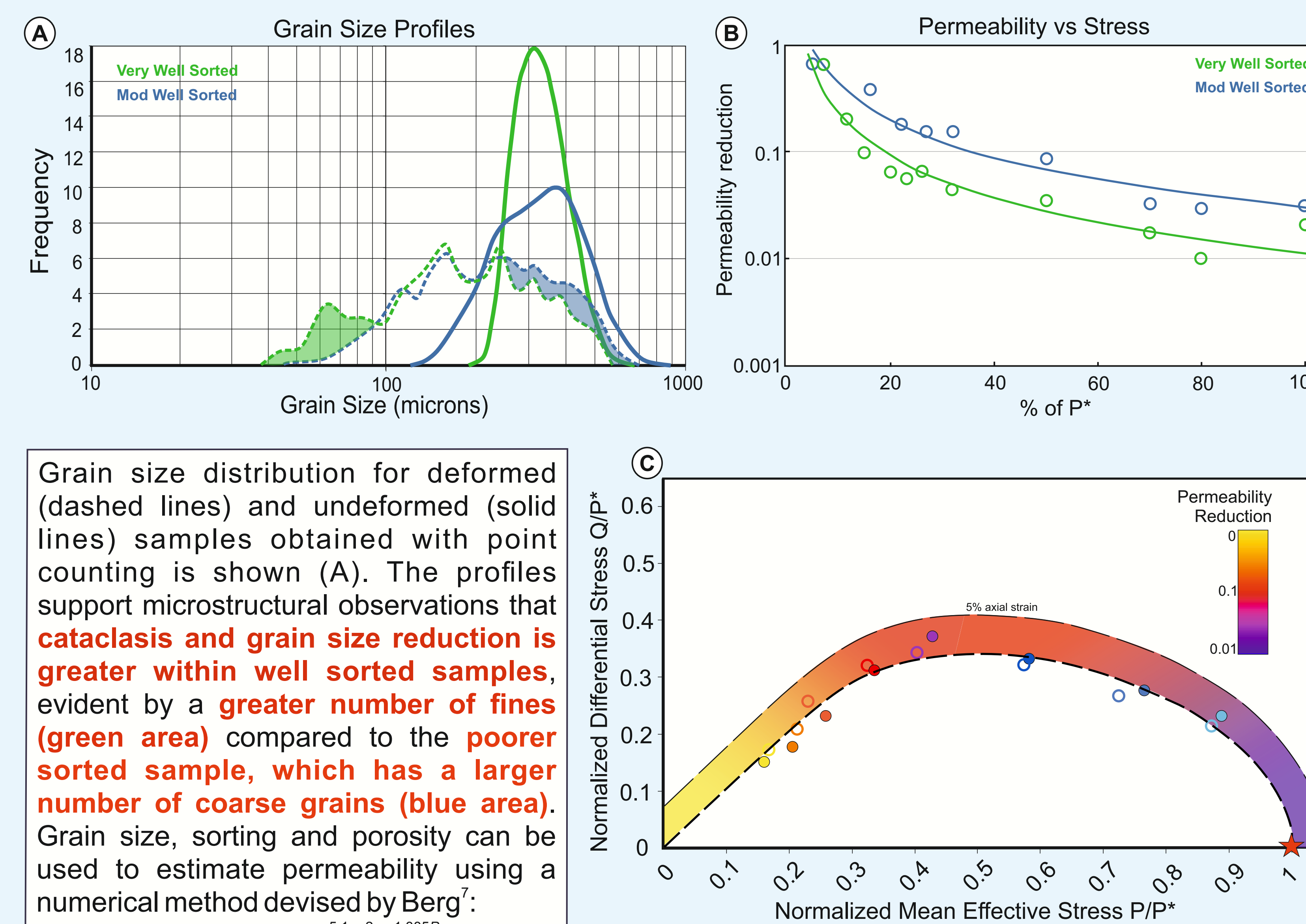


6 Band Localisation



Localised cataclasis can be observed within well sorted sands, where heavily fractured grains show some alignment at mid-high angles to the principle stress σ_1 (Figure 6a). By comparison, **poorer sorted samples display distributed pockets of cataclasis** (Figure 6c). We attribute this to the potential connectivity of force chains in accordance with the hertzian fracture model⁵ and constrained comminution⁶. In well sorted samples hertzian fracturing is easily achieved due to the connectivity of similar sized grains. In poorly sorted samples, the connectivity of similar sized grains is reduced, and fracturing restricted (6b).

7 Grain Size & Permeability Evolution



Grain size distribution for deformed (dashed lines) and undeformed (solid lines) samples obtained with point counting is shown (A). The profiles support microstructural observations that **cataclasis and grain size reduction is greater within well sorted samples**, evident by a **greater number of fines** (green area) compared to the **poorer sorted sample, which has a larger number of coarse grains** (blue area). Grain size, sorting and porosity can be used to estimate permeability using a numerical method devised by Berg⁷:

$$k = 80.8 \phi^{5.1} d^{1.385P}$$

Where k is permeability in mD, ϕ is porosity, d is mean grain size, and P is a sorting term. **Relative permeability reduction is plotted versus stress** for both very well, and moderately well-sorted samples (B). Results of triaxial tests are plotted in normalised Q-P space to produce an approximately elliptical yield cap. Permeability results may then be combined to produce a picture of **permeability evolution with different stress states around the yield curve** (C).

8 Conclusions

- Deformation transitions from grain chipping and flaking to hertzian contact fracturing and intense cataclasis with higher mean effective stress.
- Cataclasis is more intense within well sorted sands, resulting in high grain size reduction. Whilst in poorly sorted samples, cataclasis is restricted to finer grains of similar size in accordance with Sammis' constrained comminution model, leaving larger grains relatively intact.
- Grain boundary sliding may be a secondary mechanism for deformation within poorly sorted sands (inset), accounting for seemingly reduced P^* values, and less cataclasis and grain size reduction.
- Localised deformation in the form of deformation bands is favoured within well sorted sands due to connectivity of grains of similar size.
- Grain size distributions produced by deformation inevitably result in significant reduction in permeability. Well-sorted sands are most severely affected, with up to 2 orders of magnitude reduction due to significant grain size reduction. Poorly-sorted sands are reduced less so due to an overall coarser deformed grain texture.
- These results highlight the importance of understanding the effect of grain sorting on the deformation mechanisms, band formation and permeability impacts within sandstones.